ACS APPLIED MATERIALS & INTERFACES

Research Article

www.acsami.org

Visible-Light-Assisted Electrocatalytic Oxidation of Methanol Using Reduced Graphene Oxide Modified Pt Nanoflowers-TiO_2 Nanotube Arrays

Chunyang Zhai,[†] Mingshan Zhu,*[,†,‡] Duan Bin,[†] Huiwen Wang,[†] Yukou Du,*[,†] Chuanyi Wang,*[,§] and Ping Yang[†]

[†]College of Chemistry, Chemical Engineering and Materials Science, Soochow University, Suzhou 215123, P.R. China

[‡]Institute of Chemistry, Chinese Academy of Sciences, Beijing 100190, P.R. China

[§]Xinjiang Technical Institute of Physics & Chemistry, Chinese Academy of Sciences, Urumqi 830011, P. R. China

Supporting Information

ABSTRACT: In this work, Pt nanoflowers deposited on highly ordered TiO_2 nanotube arrays (TNTs) by modification of reduced graphene oxide (RGO) nanostructures have been synthesized. The ternary complex (Pt-TNTs/RGO) displays efficient electrocatalytic performance toward methanol oxidation in alkaline medium. The electrochemical impedance spectroscopy (EIS) and responsive photocurrent results indicate that the presence of graphene could effectively promote charge separation during electrocatalytic process. Interestingly, with assistance of visible light illumination, the electrocatalytic activity and stability of the ternary complex electrode toward methanol oxidation are distinctly improved. Both electro- and photo-catalytic processes for methanol oxidation contribute to the enhanced catalytic performance and stability. Moreover, the ternary electrode also displays efficient photoelectrocatalytic degradation of methylene blue (MB) under visible light illumination. The present work sheds light on developing highly efficient and long-term stability catalysts for methanol oxidation with assistance of visible-light illumination.

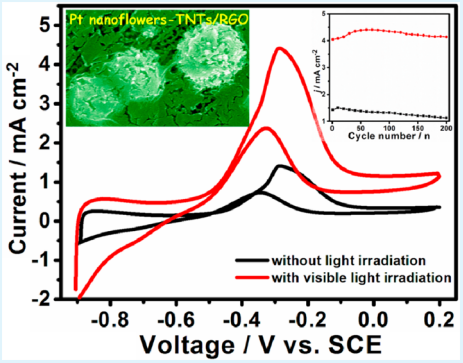

KEYWORDS: *visible-light, electrocatalytic oxidation, TiO_2 nanotubes, graphene, Pt nanoflowers*

INTRODUCTION

Fuel cells such as direct methanol fuel cells (DMFCs), as techniques for direct conversion of the chemical energy of a fuel into electrical energy with high utilization efficiency and low polluting emissions.[1−5] It is known that Pt has been acted as the most effective electrocatalyst for the anodic oxidation of fuels.[1−7] However, there are two main problems should be considered for cope with the commercialization of fuel cells in near future.[4−7] One is that pure Pt catalyst tends to get poisoned by carbon monoxide (CO). This will lead to a rapid deactivation of Pt catalyst in the electro-oxidation of methanol and hinders its technological viability. The other is high amount of Pt usage and the expensive nature of the noble metal impeding its practical viability.

To mitigate the above poisoning and cost effect, great efforts have been input over the past decades, in which the selection of a carrier for Pt electrocatalyst is one of key importance to both high catalytic performance and low cost.[4−7] To date, various combinations with different supports, such as metal oxide (such as TiO_2), carbon materials, polymer, or other supports have been developed.[4,6−12] Particularly, using TiO_2 or composited TiO_2 hybrid as catalyst support has received considerable attentions owning to its co-catalytic activity, chemical stability, corrosion resistance, low cost and ecofriendly.[9−15] Recently, some researchers found that the one-dimensional (1D) well-aligned TiO_2 nanotube arrays (TNTs) as Pt support displayed superior catalytic activity for electro-oxidation of methanol compared with conventional TiO_2 samples.[16−18] It is due to the fact that the ordered structure of TNTs provides a unidirectional electronic channel and reduces the grain boundaries.[18] Accordingly, the 1D highly ordered TNTs could be used as promising catalysts support to improve the electrocatalytic performance and stability.

On the other hand, it is well-known that the TiO_2 species has powerful oxidation under UV light excitation and is widely used as a photocatalyst for various photocatalytic applications. Accordingly, it has also reported that the presence of TiO_2 could enhance the methanol electro−oxidation performance of the electrocatalyst with assistance of UV light illumination.[10−15] Moreover, some researchers found that TiO_2-based electrocatalysts in electrocatalytic oxidation of methanol have high catalytic performance as well as self-cleaning ability.[19−22]

Received: July 1, 2014
Accepted: October 2, 2014
Published: October 2, 2014

However, the above explorations are only limited to UV light effect because of the wide band gap of TiO_2 (ca. 3.2 eV). It is well-known that ca. 45% of solar energy is visible light, whereas ca. 5% is UV light.[23] However, visible-light-assisted electrocatalytic oxidations of fuel cells have been hitherto rarely reported.

Currently, to improve the catalytic performance of the Pt-TiO_2 nanostructure, an effective method is hybridized its with various carbon materials.[24,25] For example, Wang's group successfully synthesized Pt nanoparticles deposited on the mixture of carbon black and TNTs (Pt/C-TNTs) via microwave-assisted polyol process.[24] Compared to Pt/C-TiO_2 nanoparticles and the commercial Pt/C, the Pt/C-TNTs exhibited better catalytic activity and durability in the methanol electrocatalytic oxidation reaction. Besides the carbon black, graphene, as a promising carbon material, is often used as catalysts support and promoter. This is owing to its larger specific surface area, excellent optical transmittance, high chemical, and thermal stability and outstanding electrical conductibility.[26] Furthermore, by hybridization with TiO_2 composites, graphene could endow TiO_2−graphene hybrids with visible light response for catalytic oxidation of organic molecules.[27−29] These findings inspired us to explore the potential application of graphene modified TNTs for enhanced electrocatalytic activity and stability of methanol oxidation with the aid of visible light irradiation.

Herein, in this work, we synthesized TNTs decorated with Pt nanoflowers (Pt-TNTs) and followed by modification of reduced graphene oxide nanosheets (Pt-TNTs/RGO), as shown in Scheme 1. The ternary complex displays higher electrocatalytic performance of methanol oxidation compared to Pt nanoflowers decorated TNTs in an alkaline medium. Interestingly, the electrocatalytic activity and stability of methanol oxidation could be distinctly improved with assistance of visible light illumination. Both electro- and photo-catalytic processes for methanol oxidation contribute to the enhanced catalytic performance and stability. The present work might offer a new paradigm for developing efficient yet long-term stability catalysts for DMFCs application with assistance of visible-light illumination.

Scheme 1. Schematic Illustration of the Formation Process of Pt Nanoflowers Decorated TNTs by Modification of RGO Sheets

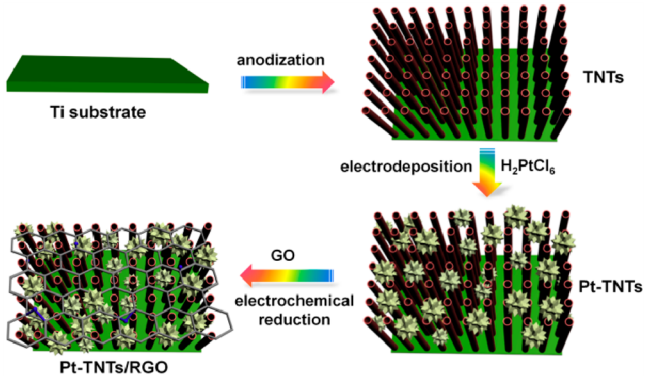

EXPERIMENTAL SECTION

Materials. Titanium (Ti) foils (10 mm × 20 mm × 0.5 mm, 99.5% purity) were supplied by Borui Titanium Industry Co., Ltd., China. All chemical reagents were purchased from Sinopharm Chemical Reagent Co., Ltd. and used without further purification. High-purity deionized (DI) water was used throughout the experiments.

Preparation of Graphene Oxide (GO) Nanosheets. GO nanosheets were obtained by chemical exfoliation of graphite with a modified Hummers' method.[8]

Synthesis of Highly Ordered TiO_2 Nanotube Arrays (TNTs). Highly ordered TiO_2 nanotube arrays (TNTs) electrode was obtained by anodic oxidation at room temperature according to the previous method.[30−32] Generally, anodization to form TiO_2 tubes arrays (TNTs) is carried out by applying a potential step at a constant voltage between 1−30 V in aqueous electrolyte or 5−150 V in nonaqueous electrolytes.[33] Prior to anodization, the pure metallic Ti foil was cleaned for 15 min in ultrasonic bath, followed by cleaning solvents in aqua regia (HNO_3:HCl, 1:3), ethanol, acetone and water for 10 min, respectively, and then dried in ambient condition. The highly ordered TNTs were fabricated by anodization of metallic Ti foil in electrolyte including ethylene glycol (98.5 v%) solution with additions of 0.3 wt % (ca. 1 g) NH_4F and 1.5 v% DI water. In detail, the as-prepared Ti foil was first immersed in 30 mL of above fresh electrolyte. Then the metallic Ti foil was used as anode and subjected to potentiostatic anodization in two electrodes configuration containing a cathode of Pt foil at 60 V for 2 h. Finally, the anode was taken out of electrolyte and rinsed immediately with DI water thoroughly and then dried in an oven at room temperature. To induce the crystalline phase, we annealed the as-synthesized TNTs at 450 °C in air for 2.5 h. The amount of as-prepared TNTs was ca. 4 mg.

Pt Nanoflower Deposited TNTs (Pt-TNTs) and Corresponding Reduced Graphene Oxide Modified Pt-TNTs (Pt-TNTs/RGO) Electrodes. The Pt nanoflowers deposited TNTs electrode was obtained by electrodeposition of Pt at −0.2 V in an aqueous solution consisting of 3.0 mM H_2PtCl_6 and 0.5 M H_2SO_4 according to a previously reported method.[8] Presuming the current efficiency is 100%, the amount of Pt loading on TNTs was measured by the charge integrated during the Pt deposition.[34] The charge for the deposition of Pt was ca. 0.32 C corresponding to the Pt loadings of 0.5 mg cm^{-2}.

The Pt-TNTs/RGO electrode was synthesized as following: 100 μL of an aqueous solution of GO (1 mg mL^{-1}) was dribbled onto the upper surface of as-synthesized Pt-TNTs electrode and dried under ambient condition. Then, bias voltage at −0.9 V vs SCE for 1500 s in sodium phosphate buffer solution (Na−PBS, 1.0 M, pH 4.2) was applied to electrochemical reduction GO, resulting in Pt-TNTs/RGO electrode. The as-synthesized electrode was washed with DI water and dried in ambient condition. The weight ratio of RGO, Pt, and TNTs in as-prepared Pt-TNTs/RGO was 1:6:40.

Electro- and Photo-electrochemical Measurements. The electro- and photo-electrochemical measurements were measured on a standard three-electrode cell using a CHI 660B potentiostat/galvanostat (Shanghai Chenhua Instrumental Co., Ltd., China) at room temperature, wherein the TNTs, Pt-TNTs, or Pt-TNTs/RGO electrode served as the working electrode. The area of working electrode was ca. 1.2 cm^2. The Pt wire and saturated calomel electrode (SCE) were worked as counter and reference electrodes, respectively. The electrochemical impedance spectroscopy (EIS) was recorded in the potentiostatic mode with the assistance of ZPlot/ZView software under an ac perturbation signal of 5 mV. The photocurrent measurement was carried out in a quartz beaker in the presence of 0.1 M Na_2SO_4 aqueous solution as the electrolyte. The working electrode was irradiated under a Xe arc lamp (150 W) during the measurement.

Electrocatalytic or Photoassisted Electrocatalytic Oxidation of Methanol. The electrocatalytic oxidation of methanol was carried out by electrochemical workstation in a three−electrode system where the as-synthesized electrode was used as the working electrode. The area of working electrode was 1.2 cm^2. The Pt wire and saturated calomel electrode (SCE) were served as counter and reference electrodes, respectively. Prior to each electrochemical measurement, the electrodes were processed by potential cycling in aqueous solution of KOH (0.5 M) in the range of −0.9 to 0.2 V until a stable state was reached. Cyclic voltammetry characteristics of the anodic electrodes

were monitored in CH_3OH (1.0 M) and KOH (0.5 M) solution. The photoassisted electrocatalytic oxidation of methanol was carried out under visible-light irradiation. A 150 W Xe arc lamp equipped with UV cut-off filter (>400 nm) was utilized as the visible−light source. To avoid the thermal effect of the reactor during light irradiation, a water channel (length × width × height = 30 cm × 10 cm × 20 cm) was put between the Xe arc lamp and the reactor and the distance of lamp to the reactor is ca. 30 cm. The integrated visible-light intensity was measured to be ca. 2.7 mW cm^{-2} by a visible-light radiometer (model FZ−A, China).

All photo or electro−chemical measurements were performed on a CHI 660B electrochemical workstation at room temperature.

Photoelectrocatalytic (PEC) Degradation of Methylene Blue (MB). The PEC performance of the as-prepared electrode was evaluated by degradation of methylene blue (MB) pollutants. A 150 W xenon arc lamp was utilized as the light source. The light passed through a water filter and a UV cut−off filter (>400 nm) before entering the reactor. Typically, working electrode (1.2 cm^2) was immersed in the aqueous solution of MB (5 mg L^{-1}, 10 mL) with a −0.3 V bias potential under visible−light irradiation. Prior to PEC process, the solution was stirred continuously for 30 min in dark room to ensure the establishment of an adsorption−desorption equilibrium. The concentration of the MB solution was recorded via a UV−vis spectrophotometer at 664 nm. C is the concentration of MB at a real−time t, and C_0 is the concentration of MB solution prior to reaction. The photocatalytic experiment (PC) or electrocatalytic experiment (EC) was carried out using the same system without applying an external potential or at the identical bias potential without light irradiation, respectively.

Characterization. The scanning electron microscope (SEM) measurements were performed by using a Hitachi S-4700 system. The X-ray diffraction (XRD) measurements were carried out by a PANalytical X′ Pert PRO MRD system with Cu Ka radiation operated at 40 kV and 30 mA. Horiba EMAX X-act energy-dispersive spectroscope was used for determined the energy dispersive X-ray (EDX). UV−vis diffuse reflectance spectra were performed on a spectrophotometer (UV−Vis−NIR Shimadzu UV3150). The Raman spectra were recorded on a Renishaw Invia Plus Raman microscope using a 633 nm argon ion laser as excitation source. The degradation of the MB molecule was monitored by measuring the real−-time UV−vis spectra of the catalytic systems using a TU-1810 UV−vis spectrophotometer (Beijing Purkinje General Instrument Co.). All of the measurements were carried out at room temperature.

RESULTS AND DISCUSSION

Experimentally, the highly ordered TNTs were obtained by anodization method. As shown in Figure 1, the highly ordered,

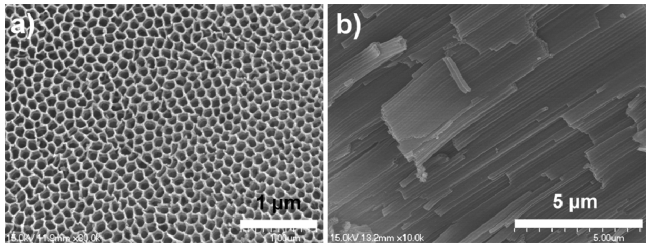

Figure 1. SEM images of (a) top and (b) cross-sections of as-synthesized TNTs nanostructures.

vertically aligned TiO_2 nanotubes were formed on the Ti substrate with nanotubes diameter of ca. 100 nm. Pt nanoflowers were deposited on the surface of TNTs according to previously described electrodeposition method,[8] resulting Pt nanoflowers decorated TNTs (Pt-TNTs). By adding graphene oxide (GO) aqueous dispersion and using potentiostatic reduction method, the RGO-modified Pt-TNTs nanostructures were successfully obtained (Pt−-TNTs/RGO). The SEM images of Pt nanoflowers decorated TNTs and Pt-TNTs/RGO nanostructures are shown in Figure 2. It can be seen that

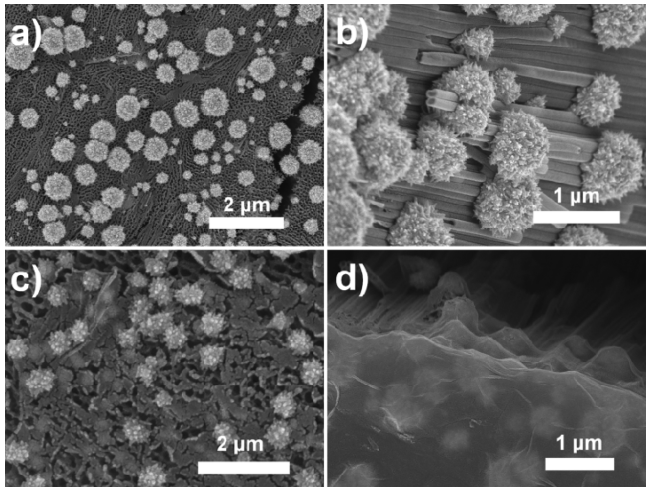

Figure 2. SEM images of (a, b) Pt-TNTs and (c, d) Pt-TNTs/RGO nanostructures.

flowers−like nanostructures ranged from 200−800 nm are dispersed on the top surface and cross−section of the TiO_2 nanotubes (Figure 2a, b). When RGO modified with Pt-TNTs nanostructure, the gauzelike graphene sheets are coated the top and cross-section of the Pt-TNTs (Figure 2c and 2d).

The composition of the TNTs, Pt-TNTs, and Pt-TNTs/RGO composites were analyzed by EDX experiment, as shown in Figure S1 in the Supporting Information. After anodization of Ti substrate, O element is detected, which confirms the formation of TiO_2 nanostructures. Compared to the theoretic stoichiometric atomic ratio, the semiquantitative analysis of the atomic ratio between Ti and O element is slightly lower. This is because of the residual metallic Ti of Ti substrate. When Pt nanoflowers were deposited on the surface of TNTs, the Pt element was detected, whereas for RGO-sheet-modified Pt-TNTs, C, O, Pt, and Ti elements were observed, indicating the presence of RGO in Pt-TNTs/RGO electrode.

The crystal structure of TNTs, Pt-TNTs, and Pt-TNTs/RGO electrodes were determined by XRD. As shown in Figure 3, the peaks at 25.3, 37.1, 37.9 48.0, 53.9, and 55.1° could be

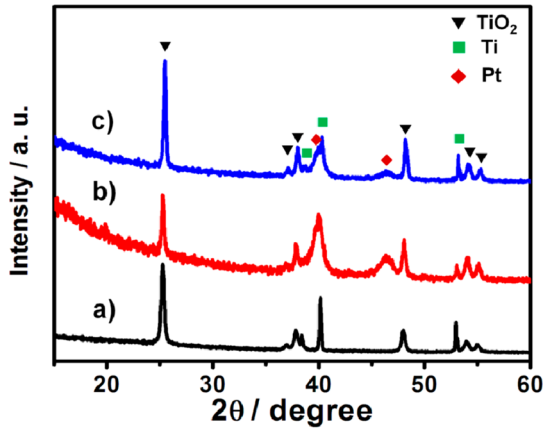

Figure 3. XRD patterns of (a) TNTs, (b) Pt-TNTs, and (c) Pt-TNTs/RGO nanostructures.

assigned to the diffraction of the (101), (103), (004), (200), (105), and (211) crystal planes of anatase TiO_2 (JCPDS No. 21−1272), respectively.[31,35,36] The other peaks of 38.5, 40.1, and 53.0° correspond to the diffraction of the (002), (101), and (102) crystal planes of Ti metal (JCPDS NO. 44−1294), respectively.[31,35] Note that in case of Pt nanoflowers deposited on the surface of TNTs, 39.7 and 46.3° peaks assigned to the diffraction of the (111) and (200) crystal planes of Pt (JCPDS NO. 04−0802), respectively, are observed.[13] However, no apparent peaks for graphene are observed in Pt−TNTs/RGO sample. This is possibly due to that the main characteristic peak of RGO (ca. 25°) has a low intensity and overlap with the peak of anatase TiO_2 at 25.3°. Similar results were also reported by others.[27−29,35] Furthermore, Raman spectra confirm the generation of anatase phase of the TNTs-based electrodes and the formation of RGO sheets in Pt-TNTs/RGO electrode, as described and shown in Figure S2 in the Supporting Information.

The UV−vis diffuse reflectance absorption spectra of as−synthesized TNTs, Pt−TNTs and Pt−TNTs/RGO composite are supplied in Figure S3 in the Supporting Information. The samples exhibited absorption in the range of 380−800 nm. Interestingly, after modification by RGO, an obvious red shift of the absorption edge is observed for the Pt−TNTs/RGO composite (417 nm) compared to the bare TNTs electrode (394 nm). A red shift of the absorption edge (23 nm) was obviously observed. This might be due to the interaction between RGO and TNTs, which is similar to what previously reported by others researches.[27−29] The Raman spectra (see Figure S2 in the Supporting Information) of the Pt-TNTs/RGO nanostructures demonstrate the interaction between RGO and TNTs. The enhanced visible light absorption implies that the present electrode might have potential application as visible-light-energized catalysts for catalytic oxidation of methanol.

To evaluate the electrochemical performance of as-synthesized electrodes, the electrochemically active surface areas (ECSAs) of Pt-TNTs and Pt-TNTs/RGO nanostructures were compared as derived by a calculation of the hydrogen desorption area from cyclic voltammograms (CV) in KOH (0.5 M) solution. Generally, the larger ECSAs mean the catalysts possess more active sites in electrocatalytic process. As shown in Figure 4 and summarized in Table 1, the ECSAs for Pt-TNTs/RGO (0.81 cm^2 mg^{-1}) is much larger than bare Pt−TNTs (0.32 cm^2 mg^{-1}). Usually, the ECSAs accounts for the catalyst surface available for charge transfer and includes the access of a conductive path to transfer the electrons to and from the electrode surface.[37] Accordingly, the large specific surface area and high conductivity of graphene leading to more effective electron and ion transport for the Pt-TNTs/RGO electrode compared with Pt-TNTs. This result also indicates that the RGO-based nanostructures might have potential application as efficient electrocatalysts for the oxidation of methanol.

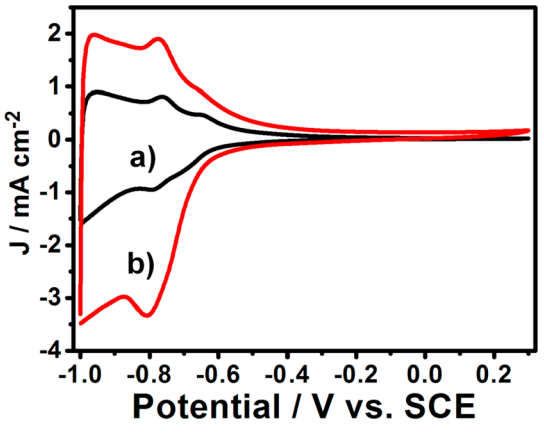

Figure 4. Cyclic voltammograms of (a) Pt-TNTs and (b) Pt-TNTs/RGO in KOH (0.5 M) solution at a scan rate of 50 mV s^{-1}.

The electrocatalytic activities of as-prepared electrodes were evaluated by cyclic voltammetry in a KOH (1.0 M) and methanol (0.5 M) solution at a scan rate of 50 mV s^{-1}. As shown in Figure 5, except the bare TNTs, the curves show typical methanol oxidation peaks at −0.29 V on Pt-based catalysts. The current densities and corresponding oxidation peak potential are summarized in Table 1. It can be seen that the bare TNTs (curve a) and TNTs/RGO (curve b) have negligible electrocatalytic ability toward methanol oxidation. When Pt nanoflowers are deposited on the surface of TNTs, the peak current density of methanol oxidation is evaluated to be ca. 1.03 mA cm^{-2}. However, for Pt−TNTs/RGO electrocatalyst, the peak current density is enhanced to be ca. 1.36 mA cm^{-2}, which is higher than that on Pt−TNTs electrode.

The above results suggest that the electrochemical activity toward methanol oxidation of the Pt-TNTs electrode could be efficiently improved by the introduction of RGO. This might be due to the excellent electronic mobility of RGO nanosheets in the ternary complexes. To test this, the electrochemical impedance spectroscopy (EIS) spectra of the electrodes were examined to verify the improvement of electron transfer efficiency. Generally, the smaller semicircle arc in the high−frequency region indicates faster interfacial charge transfer.[38,39] EIS experiments were conducted from 100 kHz to 0.1 Hz in order to investigate the internal resistance and capacity of the electrode. As shown in Figure 6, the radius of semicircle arc of the Pt−TNTs/RGO electrode is much smaller than that of TNTs electrode. Because the radius of the arc on the EIS spectrum reflects the reaction rate occurring at the surface, it clearly suggests that the separation efficiency is improved through the RGO nanosheets.

The photocurrent response is usually not only used to evaluate the charge separation efficiency in electrode, but also used to evaluate the effective separation of photogenerated electron−hole pairs. As shown in Figure 7, the photocurrent densities of the as−prepared electrodes were followed by current time (I−t) curves. The light irradiation was periodically interrupted to obtain the light current and dark current densities. When bare TNTs electrode is under light irradiation, responsive photocurrent with ca. 0.48 mA cm^{-2} is generated (Figure 7, curve a). While the Pt-TNTs and Pt-TNTs/RGO electrodes are used as working electrodes, the responsive photocurrent reaches to ca. 0.95 and 2.73 mA cm^{-2} (curve b and c), respectively. Accordingly, the photocurrent of Pt−TNTs/RGO electrode is approximately 5.7 and 2.9 times higher than that of bare TNTs and Pt−TNTs electrode, respectively. This distinctly enhanced photocurrent might be ascribed to the introduction of graphene in the Pt-TNTs/RGO system, which gives rise to a faster charger transfer and separation efficiency of the photogenerated electron−hole pairs in the Pt-TNTs/RGO.

The photoluminescence and decay data of the TNTs, Pt-TNTs, and Pt-TNTs/RGO were investigated, as shown in

Table 1. Summarization of the Electrocatalytic Performances of our Pt-Based Catalysts toward the Oxidation of CH_3OH in Alkaline Medium

electrode	Pt loading/wt % vs total support	ECSA ($cm^2\ mg^{-1}\ Pt^{-1}$)	peak potential (V) (without light)	current density ($mA\ cm^{-2}$) (without light)	peak potential (V) (with light)	current density ($mA\ cm^{-2}$) (with light)
Pt-TNTs	0.12	0.32	−0.29	1.03		
Pt-TNTs/RGO	0.12	0.81	−0.29	1.36	−0.29	4.4

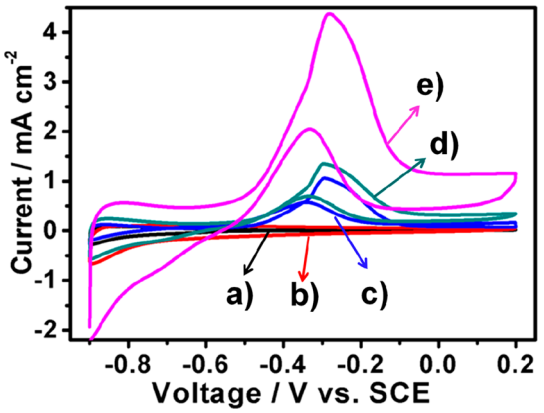

Figure 5. (a) CVs of TNTs, (b) TNTs/RGO, (c) Pt-TNTs, (d) Pt-TNTs/RGO electrode without light irradiation, and (e) Pt-TNTs/RGO electrode with visible-light irradiation in CH_3OH (1.0 M) and KOH (0.5 M) solution at a scan rate of 50 mV s^{-1}.

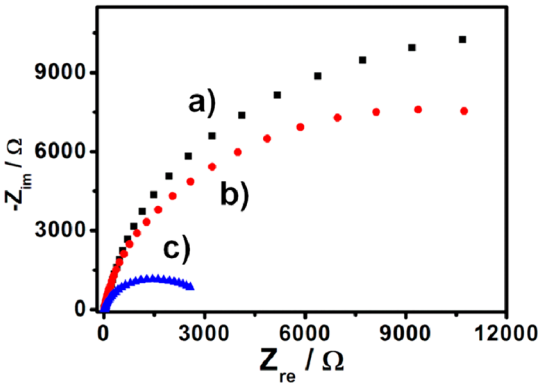

Figure 6. EIS spectra of (a) TNTs, (b) Pt-TNTs, and (c) Pt-TNTs/RGO electrode in 2.5 mM $K_3[Fe(CN)_6/K_4[Fe(CN)_6]$ and 0.1 M KCl solution at a potential of 0.3 V.

Figure S5 in the Supporting Information. First, Figure S5A in the Supporting Information shows the photoluminescence spectra of TNTs-based electrodes excited at 320 nm at room temperature. The photoluminescence spectra of all samples show the emission TNTs 465 nm, which is similar to others report.[40] However, it found that the introduction of Pt and RGO led to obvious fluorescence quenching of Pt-TNTs and Pt-TNTs/RGO samples compared with bare TNTs. This result indicated that the recombination of photoinduced electrons and holes was suppressed for Pt-TNTs and Pt-TNTs/RGO.[41] The reason for this fluorescence quenching might attribute to Pt and graphene as good electron acceptors, which could provide an efficient electron transfer pathway for deactivating the excited state TiO_2.[40] The photoluminescence decay is an important parameter to examine the charge transfer dynamics of materials in optoelectronic applications. Figure S5B in the Supporting Information and Table 2 reveal that the photoluminescence decay and corresponding kinetic constants of the

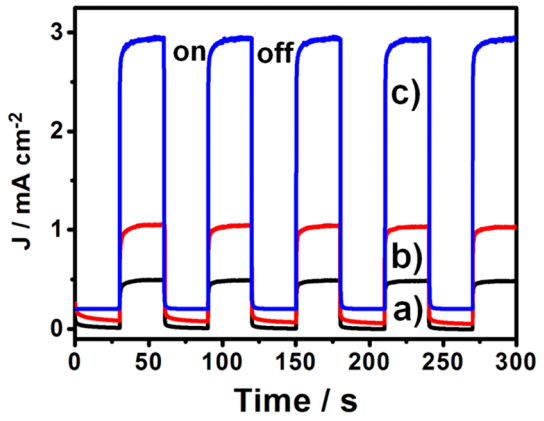

Figure 7. Photocurrent responses of (a) TNTs, (b) Pt-TNTs, and (c) Pt-TNTs/RGO electrode under light irradiation in 1.0 M CH_3OH + 0.5 M KOH solution recorded at −0.3 V. The illumination from a Xe lamp was interrupted every 30 s.

Table 2. Kinetic Constants Extracted from the Photoluminescence Decay Profiles

electrode	lifetime (μs)	mean lifetime (μs)	χ^2
TNTs	1.03 (63.93%) + 8.35 (36.07%)	3.67	0.844
Pt-TNTs	1.00 (66.47%) + 7.24 (33.53%)	3.09	0.996
Pt-TNTs/RGO	1.05 (71.27%) + 4.50 (27.73%)	2.04	0.700

TNTs, Pt-TNTs and Pt-TNTs/RGO excited at 320 nm wavelength. The mean fluorescence lifetimes of TNTs, Pt-TNTs and Pt-TNTs/RGO are 3.67, 3.09, and 2.04 μs, respectively. This result implies that during to the charge transfer process, there exists an additional channel to reduce the recombination probability, and leads to the reduction of the photogenerated carrier lifetime.[40] The electron transfer rate (k_{ET}) listed in Table 2 is calculated according to the following equation[42,43]

$$k_{ET} = \tau_{Pt-TNTs/RGO}^{-1} - \tau_{Pt-TNTs}^{-1} \quad (1)$$

where $\tau_{Pt-TNTs/RGO}^{-1}$ and $\tau_{Pt\text{-}TNTs}$ are the mean fluorescence lifetime of the Pt-TNTs and Pt-TNTs/RGO, respectively. The k_{ET} is $1.66 \times 10^5\ s^{-1}$ for Pt−TNTs/RGO. The rapid electron transfer rate is attributed to that the graphene work as electron acceptor for improving charger separation in the nanocomposites.

Compared with the electrocatalytic oxidation of methanol, an interesting phenomenon observed when the electrocatalytic process was conducted under visible light illumination. As shown in Figure 5 and summarized in Table 1, the catalytic performances toward methanol oxidation of electrodes are distinctly improved with assistance of light illumination. The current density of methanol oxidation of the Pt-TNTs/RGO

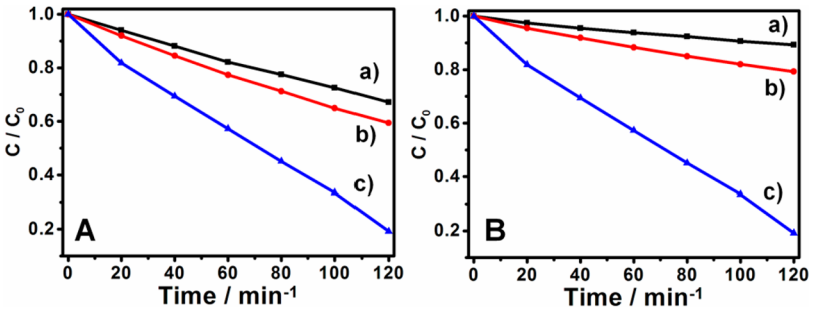

Figure 8. (A) PEC activities of (a) TNTs, (b) Pt-TNTs, and (c) Pt-TNTs/RGO for degradation of MB pollutants under visible-light illumination. (B) The degradation of MB solution over Pt−TNTs/RGO electrode using different degradation processes: (a) EC process, (b) PC process, and (c) PEC process.

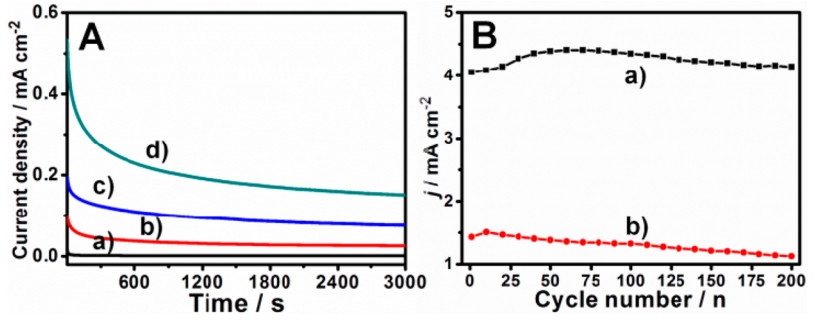

Figure 9. (A) Chronoamperometric curves of (a) TNTs, (b) Pt-TNTs, (c) Pt-TNTs/RGO electrode without light irradiation and (d) Pt-TNTs/RGO electrode with visible-light irradiation. (B) Peak current of methanol oxidation in the forward scan on Pt-TNTs/RGO electrode vs the CV cycle number (a) with or (b) without visible−light irradiations.

electrode is enhanced to 4.4 mA cm^{-2}. Compared to Pt-TNTs and Pt-TNTs/RGO nanostructures without light irradiation, the catalytic oxidation of methanol performance is improved by 4.3 and 3.2 times with assistance by visible-light irradiation, respectively. It could be due to a synergetic effect of electrocatalysis and photocatalysis during methanol oxidation process. Accordingly, the photoassisted electrocatalytic process could remarkably enhance the oxidation efficiency toward methanol oxidation.

In addition, the electrocatalytic activity of the Pt-TNTs and Pt-TNTs/RGO electrodes with and without light irradiation in acid medium were also studied in the results are supplied in Figure S4 in the Supporting Information. All samples show obvious forward peak current at about 0.7 V for methanol oxidation. The anodic peak density of Pt-TNTs/RGO (4.45 mA cm^{-2}) is higher than that of the Pt-TNTs (2.64 mA cm^{-2}) without light irradiation, demonstrating that the introduction of graphene enhances the electrocatalytic activity. Compared to Pt−TNTs and Pt-TNTs/RGO nanostructures without light irradiation, the catalytic oxidation of methanol performance is improved by 4 and 2.37 times with assisted of visible light irradiation for Pt-TNTs/RGO electrode (10.55 mA cm^{-2}), respectively. Therefore, this result is similar to the photoelectrocatalytic oxidation of methanol in an alkaline medium, in which photoassisted electrocatalytic process could enhance the catalytic efficiency toward methanol oxidation.

To investigate the superiority of the photoelectrocatalytic (PEC) process of the Pt-TNTs/RGO electrode, the removal of MB pollutants by as-prepared electrode and with the various degradation processes (viz. electrochemical (EC), photocatalytic (PC), and PEC process) were studied, as shown in Figure 8. First, ca. 80.9% of MB pollutants are degraded when Pt−TNTs/RGO is used as catalysts after 120 min visible-light irradiation (Figure 8A). This is distinctly higher than that of bare TNTs (ca. 32.8%) and Pt−TNTs (ca. 40.6%) electrode acted as the working electrode for PEC degradation of MB pollutant, respectively. The corresponding turnover frequencies (TOFs) of Pt-TNTs/RGO, Pt-TNTs, and TNTs electrodes were 4.3 × 10^{-3} h^{-1}, 2.21 × 10^{-3} h^{-1}, and 2.05 × 10^{-3} h^{-1}, respectively. On the other hand, compared with other degradation process, the PEC process (80.9%) shows the highest degradation efficiency among these processes (Figure 8B), where the EC process and PC process only degraded 10.8% and 20.7% of MB molecules during the same time period, respectively. The corresponding TOFs of Pt-TNTs/RGO electrode for PEC, PC, and EC process were 4.3 × 10^{-3} h^{-1}, 1.1 × 10^{-3} h^{-1}, and 5.7 × 10^{-4} h^{-1}, respectively. The recyclability of Pt−TNTs/RGO was investigated for the degradation of MB pollutant under visible light irradiation. No significant changes in the PEC performances were observed after nine cycling runs, suggesting our Pt−TNTs/RGO could be served as a stable catalyst for the degradation of organic pollutants (refer Figure S6 in the Supporting Information for details). This result is similar to that of visible-light-assisted electrocatalytic methanol oxidation, which supports that photoassisted electrocatalysis is distinctly superior to the traditional catalytic process.

The long-term stability is another important factor for a catalyst in fuel cell practical application. To evaluate the stability of the catalysts, we first polarized the three electrodes at −0.3 V for a period of 3000 s. Figure 9A shows the chronoamperometric curves of methanol oxidation on TNTs, Pt-TNTs, and Pt-TNTs/RGO without visible-light irradiation. Compared to bare TNTs and Pt-TNTs electrodes, the maximum initial and steady−state oxidation current densities of Pt-TNTs/RGO are evidently larger. When the Pt-TNTs/

RGO electrode is under visible-light irradiation, the initial and steady-state oxidation current densities are further enhanced, indicating the catalytic activity and stability are improved by assistance of light illumination efficiently.

Furthermore, the oxidation peak current density of the Pt-TNTs/RGO electrode with long-time cycle with and without light irradiation was explored. As shown in Figure 9B, the oxidation peak current density increases at the initial stage and then keeps steady under visible light irradiation. After 200 cycles, compared with the maximum value, the peak current densities of electrode only decrease by ca. 4.5%. However, under dark environment, the peak current densities are evidently lower than the former process. Moreover, the peak current densities decrease gradually as the number of scans further increase. After 200 cycles, the peak current densities decrease by 25.3% relative to its maximum value.

The ratio of the forward anodic peak current (I_f) to the backward cathodic peak current (I_b) is often used to evaluate the catalyst tolerance to CO and other carbonaceous species.[44−46] Based inn the basis of Figure 5, the I_f/I_b values of the electrodes are summarized in Table 3. It can be seen that

Table 3. Summarized I_f, I_b, and I_f/I_b Values of our Pt-Based Catalysts toward the Oxidation of CH_3OH in Alkaline Medium

electrode	I_f (mA cm^{-2})	I_b (mA cm^{-2})	I_f/I_b
Pt-TNTs (without light)	1.05	0.57	1.84
Pt-TNTs/RGO (without light)	1.35	0.7	1.93
Pt-TNTs/RGO (with light)	4.4	2.05	2.15

compared to Pt-TNTs, the corresponding Pt-TNTs/RGO electrode exhibits higher I_f/I_b value. Moreover, with assistance of light irradiation, the I_f/I_b value of Pt-TNTs/RGO electrode was further improved. Generally, a higher ratio indicates more effective removal of the poisoning species on the catalyst surface.[45,46] This result is in aggrement with the oxidation peak current density of the Pt-TNTs/RGO electrode with long-time cycle with and without light irradiation. Accordingly, with assistance of visible-light irradiation, the electrocatalytic performances as well as catalytic stabilities in the RGO modified Pt-TNTs electrode for oxidation of methanol are improved.

On the basis of the above results, with visible-light irradiation, the electrocatalytic performances as well as catalytic stabilities in the RGO modified Pt-TNTs electrode for oxidation of methanol are distinctly improved. First, during the catalytic process, graphene as an excellent electron conductor, higher charge separation efficiency could be achieved in the Pt-TNTs/RGO electrode. Moreover, the introduction of the graphene nanosheets in Pt-TNTs/RGO nanostructures could promote the utilization of the visible-light spectrum. When the electrode is upon irradiation by visible light, an electron (e^-) is photoexcited from its valence band (VB) and leaves a hole (h^+) in the valence band (VB). When reacts with OH^-/H_2O at the surface of catalyst, the h^+ potential is positive enough to form hydroxyl radicals (•OH) on the surface of catalyst and the e^- would transport to graphene followed by transfer to the electrode (Scheme 2).[39] The hydroxyl radicals are strong oxidant species in favor of oxidizing the species (e.g., CH_3OH) adsorbed on the surface of the catalyst.[10−15] Therein, the reactive radical species could also oxidize the intermediate carbonaceous species like CO,

Scheme 2. Schematic Illustration for Photoassisted Electrocatalytic Oxidation Methanol Process by Using Pt-TNTs/RGO Electrode under Visible−light Irradiation

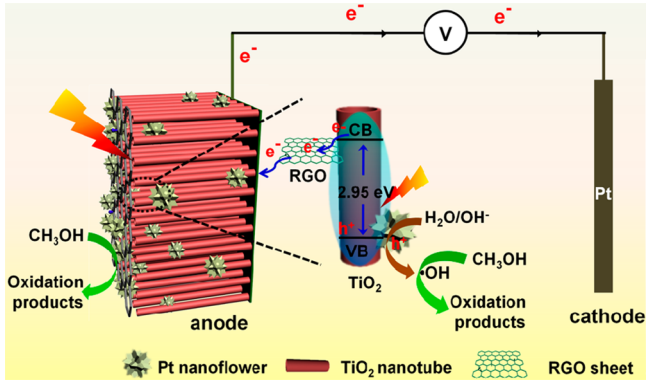

resulting in an efficiently poisoning suppression. Thus, with assistance of visible-light irradiation, the catalytic performance and stability toward oxidation of methanol of Pt-TNTs/RGO can be improved efficiently.

CONCLUSIONS

In conclusion, highly ordered TiO_2 nanotube arrays decorated with Pt nanoflowers with modification of RGO nanosheets electrode have been fabricated. The ternary complex displays high electrocatalytic activity and great stability for methanol oxidation in alkaline medium with the aid of visible light irradiation. Graphene not only improves the utilization of the solar energy but also promotes charge separation during the catalytic process. With visible-light illumination, electrocatalysis and photocatalysis both occur in the photoassisted electrocatalytic process. This work provides new opportunities for exploiting visible-light-assisted enhancement of long-term-stable and highly efficient anode catalysts for PMFCs that are expected to hold great promise in water splitting, solar cells, and other light-harvesting systems.

ASSOCIATED CONTENT

Supporting Information

EDX, UV−vis diffuse reflectance, Raman, photoluminescence spectra, and decay profile spectra of TNTs, Pt-TNTs, and Pt-TNTs/RGO nanostructures. The CVs spectra of the Pt-TNTs and Pt-TNTs/RGO electrodes under acid medium. The recyclability of Pt-TNTs/RGO catalyst for PEC degradation of MB pollutant. This material is available free of charge via the Internet at http://pubs.acs.org/.

AUTHOR INFORMATION

Corresponding Authors

*E-mail: mingshanzhu@yahoo.com.
*E-mail: cywang@ms.xjb.ac.cn.
*E-mail: duyk@suda.edu.cn.

Author Contributions

The manuscript was written through contributions of all authors. All authors have given approval to the final version of the manuscript.

Notes

The authors declare no competing financial interest.

■ ACKNOWLEDGMENTS

This work was supported by the NSFC (51373111, 51073114, 21173261 and 20933007), Suzhou Nano−project (ZXG2012022), the Priority Academic Program Development of Jiangsu Higher Education Institutions (PAPD), the Project of Scientific and Technologic Infrastructure of Suzhou (SZS201207), and the Academic Award for Young Graduate Scholar of Soochow University.

■ REFERENCES

(1) Aricò, A. S.; Srinivasan, S.; Antonucci, V. DMFCs: From Fundamental Aspects to Technology Development. *Fuel Cells* **2011**, *1*, 133−161.
(2) Liu, H. S.; Song, C. J.; Zhang, L.; Wang, H. J.; Wilkinson, D. P. A Review of Anode Catalysis in the Direct Methanol Fuel Cell. *J. Power Sources* **2006**, *155*, 95−110.
(3) Zainoodin, A. M.; Kamarudin, S. K.; Daud, W. R. W. Electrode in Direct Methanol Fuel Cells. *Int. J. Hydrogen Energy* **2010**, *35*, 4606−4621.
(4) Basri, S.; Kamarudin, S. K.; Daud, W. R. W.; Yaakub, Z. Nanocatalyst for Direct Methanol Fuel Cell (DMFC). *Int. J. Hydrogen Energy* **2010**, *35*, 7957−7970.
(5) Zhao, X.; Yin, M.; Ma, L.; Liang, L.; Liu, C.; Liao, J.; Lu, T.; Xing, W. Recent Advances in Catalysts for Direct Methanol Fuel Cells. *Energy Environ. Sci.* **2011**, *4*, 2736−2753.
(6) Cao, M. N.; Wu, D. S.; Cao, R. Recent Advances in the Stabilization of Platinum Electrocatalysts for Fuel-Cell Reactions. *ChemCatChem.* **2014**, *6*, 26−45.
(7) Huang, H. J.; Wang, X. Recent Progress on Carbon-Based Support Materials for Electrocatalysts of Direct Methanol Fuel Cells. *J. Mater. Chem. A* **2014**, *2*, 6266−6291.
(8) Yao, Z. Q.; Zhu, M. S.; Jiang, F. X.; Du, Y. K.; Wang, C. Y.; Yang, P. Highly Efficient Electrocatalytic Performance Based on Pt Nanoflowers Modified Reduced Graphene Oxide/Carbon Cloth Electrode. *J. Mater. Chem.* **2012**, *22*, 13707−13713.
(9) Zhang, H. M.; Zhou, W. Q.; Du, Y. K.; Yang, P.; Wang, C. Y.; Xu, J. K. Enhanced Electrocatalytic Performance for Methanol Oxidation on Pt-TiO_2/ITO Electrode under UV Illumination. *Int. J. Hydrogen Energy* **2010**, *35*, 13290−13297.
(10) Wu, S. C.; He, J. P.; Zhou, J. H.; Wang, T.; Guo, Y. X.; Zhao, J. Q.; Ding, X. C. Fabrication of Unique Stripe-Shaped Mesoporous TiO_2 Films and Their Performance as a Novel Photo-Assisted Catalyst Support for DMFCs. *J. Mater. Chem.* **2011**, *21*, 2852−2854.
(11) Li, W.; Bai, Y.; Li, F. J.; Liu, C.; Chan, K. Y.; Feng, X.; Lu, X. H. Core−Shell TiO_2/C Nanofibers as Supports for Electrocatalytic and Synergistic Photoelectrocatalytic Oxidation of Methanol. *J. Mater. Chem.* **2012**, *22*, 4025−4031.
(12) Lv, Q.; Yin, M.; Zhao, X.; Li, C. Y.; Liu, C. P.; Xing, W. Promotion Effect of TiO_2 on Catalytic Activity and Stability of Pt Catalyst for Electrooxidation of Methanol. *J. Power Sources* **2012**, *218*, 93−99.
(13) Mojumder, N.; Sarker, S.; Abbas, S. A.; Tian, Z.; Subramanian, V. Photoassisted Formic Acid on Platinized TiO_2 Nanotubes. *ACS Appl. Mater. Interfaces* **2014**, *6*, 5585−5594.
(14) Wang, C. Q.; Jiang, F. X.; Yue, R. R.; Wang, H. W.; Du, Y. K. Enhanced Photo-Electrocatalytic Performance of Pt/RGO/TiO_2 on Carbon Fiber towards Methanol Oxidation in Alkaline Media. *J. Solid State Electrochem* **2014**, *18*, 515−522.
(15) Wang, C. Q.; Yue, R. R.; Wang, H. W.; Zou, C.; Du, J.; Jiang, F. X.; Du, Y. K.; Yang, P.; Wang, C. Y. Dendritic Ag@Pt Coreeshell Catalyst Modified with Reduced Graphene Oxide and Titanium Dioxide: Fabrication, Characterization, and Its Photo-Electrocatalytic Performance. *Int. J. Hydrogen Energy* **2014**, *39*, 5764−5771.
(16) Song, H. Q.; Qiu, X. P.; Li, X. X.; Li, F. S.; Zhu, W. T.; Chen, L. Q. TiO_2 Nanotubes Promoting Pt/C Catalysts for Ethanol Electro-Oxidation in Acidic Media. *J. Power Sources* **2007**, *170*, 50−54.
(17) Xiao, P.; Song, H.; Zhu, W. T.; Chen, L.; Stimmingc, U.; Bele, P. Study on the Co-Catalytic Effect of Titanate Nanotubes on Pt-based Catalysts Indirect Alcohol Fuel Cells. *Appl. Catal. B: Environ.* **2010**, *197*, 204−212.
(18) Xing, L.; Jia, J. B.; Wang, Y. Z.; Zhang, B. L.; Dong, S. J. Pt Modified TiO_2 Nanotubes Electrode: Preparation and Electrocatalytic Application for Methanol Oxidation. *Int. J. Hydrogen Energy* **2010**, *35*, 12169−12173.
(19) Song, Y. Y.; Gao, Z. D.; Schmuki, P. Highly Uniform Pt Nanoparticle Decoration on TiO_2 Nanotube Arrays: A Refreshable Platform for Methanol Electrooxidation. *Electrochem. Commun.* **2011**, *13*, 290−293.
(20) Hosseini, M. G.; Momeni, M. M. UV-Cleaning Properties of Pt Nanoparticle-Decorated Titania Nanotubes in the Electro-Oxidation of Methanol: An Anti-poisoning and Refreshable Electrode. *Electrochim. Acta* **2012**, *70*, 1−9.
(21) Hosseini, M. G.; Momeni, M. M. Evaluation of the Performance of Platinum Nanoparticle−Titanium Oxide Nanotubes as a New Refreshable Electrode for Formic Acid Electrooxidation. *Fuel Cells* **2012**, *12*, 406−414.
(22) Hosseini, M. G.; Momeni, M. M. Fabrication and Photoelectrocatalytic Activity of Highly Oriented Titania Nanotube Loaded with Platinum Nanoparticles for Electro-oxidation of Lactose: A New Recyclable Electro-catalyst. *J. Mol. Catal. A: Chem.* **2012**, *355*, 216−222.
(23) Chen, C. C.; Ma, W. H.; Zhao, J. C. Semiconductor-mediated Photodegradation of Pollutants under Visible-light Irradiation. *Chem. Soc. Rev.* **2010**, *39*, 4206−4219.
(24) Sui, X. L.; Wang, Z. B.; Yang, M.; Huo, L.; Gu, D. M.; Yin, G. P. Investigation on C- TiO_2 Nanotubes Composite as Pt Catalyst Support for Methanol Electrooxidation. *J. Power Sources* **2014**, *255*, 43−51.
(25) Ruiz-Camacho, B.; Martínez-Álvarez, O.; Rodríguez-Santoyo, H. H.; Granados-Alejo, V. Pt/C and Pt/TiO_2−C Electrocatalysts Prepared by Chemical Vapor Deposition with High Tolerance to Alcohols in Oxygen Reduction Reaction. *J. Electroanal. Chem.* **2014**, *725*, 19−24.
(26) Sun, Y. Q.; Wu, Q.; Shi, G. Q. Graphene Based New Energy Materials. *Energy Environ. Sci.* **2011**, *4*, 1113−1132.
(27) Zhang, H.; Lv, X.; Li, Y. M.; Wang, Y.; Li, J. H. P25-Graphene Composite as a High Performance Photocatalyst. *ACS Nano* **2010**, *4*, 380−386.
(28) Zhang, Y. H.; Tang, Z. R.; Fu, X. Z.; Xu, Y. J. TiO_2Graphene Nanocomposites for Gas-Phase Photocatalytic Degradation of Volatile Aromatic Pollutant: Is TiO_2 Graphene Truly Different from Other TiO_2 Carbon Composite Materials? *ACS Nano* **2010**, *4*, 7303−7314.
(29) Yang, M. Q.; Zhang, N.; Xu, Y. J. Synthesis of Fullerene−, Carbon Nanotube−, and Graphene−TiO_2 Nanocomposite Photocatalysts for Selective Oxidation: A Comparative Study. *ACS Appl. Mater. Interfaces* **2013**, *5*, 1156−1164.
(30) Prakasam, H. E.; Shankar, K.; Paulose, M.; Varghese, O. K.; Grimes, C. A. A New Benchmark for TiO_2 Nanotube Array Growth by Anodization. *J. Phys. Chem. C* **2007**, *111*, 7235−7241.
(31) Dai, G. P.; Yu, J. G.; Liu, G. Synthesis and Enhanced Visible-Light Photoelectrocatalytic Activity of *p-n* Junction BiOI/TiO_2 Nanotube Arrays. *J. Phys. Chem. C* **2011**, *115*, 7339−7346.
(32) Zhai, C. Y.; Zhu, M. S.; Lu, Y. T.; Ren, F. F.; Wang, C. Q.; Du, Y. K.; Yang, P. Reduced Graphene Oxide Modified Highly Ordered TiO_2 Nanotube Arrays Photoelectrode with Enhanced Photoelectrocatalytic Performance under Visible−light Irradiation. *Phys. Chem. Chem. Phys.* **2014**, *16*, 14800−14807.
(33) Roy, P.; Berger, S.; Schmuki, P. TiO_2 Nanotubes: Synthesis and Applications. *Angew. Chem., Int. Ed.* **2011**, *50*, 2904−2939.
(34) Kuo, C. W.; Huang, L. M.; Wen, T. C.; Gopalan, A. Enhanced Electrocatalytic Performance for Methanol Oxidation of A Novel Pt-dispersed Poly(3,4-ethylenedioxythiophene)−poly(styrene sulfonic acid) Electrode. *J. Power Sources* **2006**, *160*, 65−72.
(35) Perera, S. D.; Mariano, R. G.; Vu, K.; Nour, N.; Seitz, O.; Chabal, Y.; Balkus, K. J. Hydrothermal Synthesis of Graphene-TiO_2 Nanotube Composites with Enhanced Photocatalytic Activity. *ACS Catal.* **2012**, *2*, 949−956.

(36) Yu, J. G.; Dai, G. P.; Cheng, B. Effect of Crystallization Methods on Morphology and Photocatalytic Activity of Anodized TiO_2 Nanotube Array Films. *J. Phys. Chem. C* **2010**, *114*, 19378−19385.
(37) Seger, B.; Kamat, P. V. Electrocatalytically Active Graphene-Platinum Nanocomposites. Role of 2-D Carbon Support in PEM Fuel Cells. *J. Phys. Chem. C* **2009**, *113*, 7990−7995.
(38) Adachi, M.; Sakamoto, M.; Jin, J. T.; Ogata, Y.; Isoda, S. Determination of Parameters of Electron Transport in Dye-Sensitized Solar Cells Using Electrochemical Impedance Spectroscopy. *J. Phys. Chem. B* **2006**, *110*, 13872−13880.
(39) Zhai, C. Y.; Zhu, M. S.; Ren, F. F.; Yao, Z. Q.; Du, Y. K.; Yang, P. Enhanced Photoelectrocatalytic Performance of Titanium Dioxide/Carbon Cloth Based Photoelectrodes by Graphene Modification under Visible−Light Irradiation. *J. Hazardous Mater.* **2013**, *263*, 291−298.
(40) Gu, L.; Wang, J. Y.; Cheng, H.; Zhao, Y. Z.; Liu, L.; Han, X. J. One-Step Preparation of Graphene-Supported Anatase TiO_2 with Exposed {001} Facets and Mechanism of Enhanced Photocatalytic Properties. *ACS Appl. Mater. Interfaces* **2013**, *5*, 3085−3093.
(41) Liu, J. H.; Wang, Z. C.; Liu, L. W.; Chen, W. Reduced Graphene Oxide as Capturer of Dyes and Electrons During Photocatalysis: Surface Wrapping and Capture Promoted Efficiency. *Phys. Chem. Chem. Phys.* **2011**, *13*, 13216−13221.
(42) Kongkanand, A.; Tvrdy, K.; Takechi, K.; Kuno, M.; Kamat, P. V. Quantum Dot Solar Cells. Tuning Photoresponse through Size and Shape Control of CdSe-TiO_2 Architecture. *J. Am. Chem. Soc.* **2008**, *130*, 4007−4015.
(43) Zhu, M. S.; Du, Y. K.; Yang, P.; Wang, X. M. Donor−Acceptor Porphyrin Functionalized Pt Nano-assemblies for Artificial Photosynthesis: a Simple and Efficient Homogeneous Photocatalytic Hydrogen Production System. *Catal. Sci. Technol.* **2013**, *3*, 2295−2302.
(44) Bin, D.; Ren, F. F.; Wang, H.; Zhang, K.; Yang, B.; Zhai, C.; Zhu, M. S.; Yang, P.; Du, Y. K. Facile Synthesis of PVP-Assisted PtRu/RGO Nanocomposites with High Electrocatalytic Performance for Methanol Oxidation. *RSC Adv.* **2014**, DOI: 10.1039/c4ra07742c.
(45) Mehta, S. K.; Gupta, S. Time-Efficient Microwave Synthesis of Pd Nanoparticles and Their Electrocatalytic Property in Oxidation of Formic Acid and Alcohols in Alkaline Media. *J. Appl. Electrochem.* **2011**, *41*, 1407−1417.
(46) Chen, X.; Cai, H.; Tang, Q.; He, B.; Chen, H. Eggshell Membrane Templated Y_2O_3@Pd Catalyst for Enhanced Methanol Oxidation and CO Tolerance. *Mater. Res. Innov.* **2014**, *18*, 300−306.